96. Tinsley, JM, Blake, DJ, Roche, A, Fairbrother, U, Riss, J, Byth, BC *et al.* (1992). Primary structure of dystrophin-related protein. *Nature* **360**: 591–593.
97. Tanaka, H, Ishiguro, T, Eguchi, C, Saito, K and Ozawa, E (1991). Expression of a dystrophin-related protein associated with the skeletal muscle cell membrane. *Histochemistry* **96**: 1–5.
98. Mizuno, Y, Nonaka, I, Hirai, S and Ozawa, E (1993). Reciprocal expression of dystrophin and utrophin in muscles of Duchenne muscular dystrophy patients, female DMD-carriers and control subjects. *J Neurol Sci* **119**: 43–52.
99. Tinsley, J, Deconinck, N, Fisher, R, Kahn, D, Phelps, S, Gillis, JM *et al.* (1998). Expression of full-length utrophin prevents muscular dystrophy in *mdx* mice. *Nat Med* **4**: 1441–1444.
100. Krag, TO, Bogdanovich, S, Jensen, CJ, Fischer, MD, Hansen-Schwartz, J, Javazon, EH *et al.* (2004). Heregulin ameliorates the dystrophic phenotype in *mdx* mice. *Proc Natl Acad Sci USA* **101**: 13856–13860.
101. Chaubourt, E, Fossier, P, Baux, G, Leprince, C, Israël, M and De La Porte, S (1999). Nitric oxide and l-arginine cause an accumulation of utrophin at the sarcolemma: a possible compensation for dystrophin loss in Duchenne muscular dystrophy. *Neurobiol Dis* **6**: 499–507.
102. Sonnemann, KJ, Heun-Johnson, H, Turner, AJ, Baltgalvis, KA, Lowe, DA and Ervasti, JM (2009). Functional substitution by TAT-utrophin in dystrophin-deficient mice. *PLoS Med* **6**: e1000083.
103. Squire, S, Raymackers, JM, Vandebrouck, C, Potter, A, Tinsley, J, Fisher, R *et al.* (2002). Prevention of pathology in *mdx* mice by expression of utrophin: analysis using an inducible transgenic expression system. *Hum Mol Genet* **11**: 3333–3344.
104. Miura, P and Jasmin, BJ (2006). Utrophin upregulation for treating Duchenne or Becker muscular dystrophy: how close are we? *Trends Mol Med* **12**: 122–129.
105. Li, D, Bareja, A, Judge, L, Yue, Y, Lai, Y, Fairclough, R *et al.* (2010). Sarcolemmal nNOS anchoring reveals a qualitative difference between dystrophin and utrophin. *J Cell Sci* **123**(Pt 12): 2008–2013.
106. Anderson, WF (1990). September 14, 1990: the beginning. *Hum Gene Ther* **1**: 371–372.
107. Lehrman, S (1999). Virus treatment questioned after gene therapy death. *Nature* **401**: 517–518.
108. Hacein-Bey-Abina, S, von Kalle, C, Schmidt, M, Le Deist, F, Wulffraat, N, McIntyre, E *et al.* (2003). A serious adverse event after successful gene therapy for X-linked severe combined immunodeficiency. *N Engl J Med* **348**: 255–256.
109. Aiuti, A, Cattaneo, F, Galimberti, S, Benninghoff, U, Cassani, B, Callegaro, L *et al.* (2009). Gene therapy for immunodeficiency due to adenosine deaminase deficiency. *N Engl J Med* **360**: 447–458.
110. Acsadi, G, Dickson, G, Love, DR, Jani, A, Walsh, FS, Gurusinghe, A *et al.* (1991). Human dystrophin expression in *mdx* mice after intramuscular injection of DNA constructs. *Nature* **352**: 815–818.
111. Wang, B, Li, J and Xiao, X (2000). Adeno-associated virus vector carrying human minidystrophin genes effectively ameliorates muscular dystrophy in *mdx* mouse model. *Proc Natl Acad Sci USA* **97**: 13714–13719.
112. Harper, SQ, Hauser, MA, DelloRusso, C, Duan, D, Crawford, RW, Phelps, SF *et al.* (2002). Modular flexibility of dystrophin: implications for gene therapy of Duchenne muscular dystrophy. *Nat Med* **8**: 253–261.
113. Phelps, SF, Hauser, MA, Cole, NM, Rafael, JA, Hinkle, RT, Faulkner, JA *et al.* (1995). Expression of full-length and truncated dystrophin mini-genes in transgenic *mdx* mice. *Hum Mol Genet* **4**: 1251–1258.
114. Rafael, JA, Cox, GA, Corrado, K, Jung, D, Campbell, KP and Chamberlain, JS (1996). Forced expression of dystrophin deletion constructs reveals structure-function correlations. *J Cell Biol* **134**: 93–102.
115. Wells, DJ, Wells, KE, Asante, EA, Turner, G, Sunada, Y, Campbell, KP *et al.* (1995). Expression of human full-length and minidystrophin in transgenic *mdx* mice: implications for gene therapy of Duchenne muscular dystrophy. *Hum Mol Genet* **4**: 1245–1250.
116. Gregorevic, P, Blankinship, MJ, Allen, JM, Crawford, RW, Meuse, L, Miller, DG *et al.* (2004). Systemic delivery of genes to striated muscles using adeno-associated viral vectors. *Nat Med* **10**: 828–834.
117. Wang, Z, Zhu, T, Qiao, C, Zhou, L, Wang, B, Zhang, J *et al.* (2005). Adeno-associated virus serotype 8 efficiently delivers genes to muscle and heart. *Nat Biotechnol* **23**: 321–328.
118. Wang, B, Li, J, Qiao, C, Chen, C, Hu, P, Zhu, X *et al.* (2008). A canine minidystrophin is functional and therapeutic in *mdx* mice. *Gene Ther* **15**: 1099–1106.
119. Wang, Z, Kuhr, CS, Allen, JM, Blankinship, M, Gregorevic, P, Chamberlain, JS *et al.* (2007). Sustained AAV-mediated dystrophin expression in a canine model of Duchenne muscular dystrophy with a brief course of immunosuppression. *Mol Ther* **15**: 1160–1166.
120. Ohshima, S, Shin, JH, Yuasa, K, Nishiyama, A, Kira, J, Okada, T *et al.* (2009). Transduction efficiency and immune response associated with the administration of AAV8 vector into dog skeletal muscle. *Mol Ther* **17**: 73–80.
121. Wang, Z, Storb, R, Lee, D, Kushmerick, MJ, Chu, B, Berger, C *et al.* (2010). Immune responses to AAV in canine muscle monitored by cellular assays and noninvasive imaging. *Mol Ther* **18**: 617–624.
122. Rodino-Klapac, LR, Montgomery, CL, Bremer, WG, Shontz, KM, Malik, V, Davis, N *et al.* (2010). Persistent expression of FLAG-tagged micro dystrophin in nonhuman primates following intramuscular and vascular delivery. *Mol Ther* **18**: 109–117.
123. Mendell, JR, Campbell, K, Rodino-Klapac, L, Sahenk, Z, Shilling, C, Lewis, S *et al.* (2010). Dystrophin immunity in Duchenne's muscular dystrophy. *N Engl J Med* **363**: 1429–1437.
124. Goyenvalle, A, Vulin, A, Fougerousse, F, Leturcq, F, Kaplan, JC, Garcia, L *et al.* (2004). Rescue of dystrophic muscle through U7 snRNA-mediated exon skipping. *Science* **306**: 1796–1799.
125. Denti, MA, Incitti, T, Sthandier, O, Nicoletti, C, De Angelis, FG, Rizzuto, E *et al.* (2008). Long-term benefit of adeno-associated virus/antisense-mediated exon skipping in dystrophic mice. *Hum Gene Ther* **19**: 601–608.
126. Qiao, C, Li, J, Jiang, J, Zhu, X, Wang, B, Li, J *et al.* (2008). Myostatin propeptide gene delivery by adeno-associated virus serotype 8 vectors enhances muscle growth and ameliorates dystrophic phenotypes in *mdx* mice. *Hum Gene Ther* **19**: 241–254.
127. Qiao, C, Li, J, Zheng, H, Bogan, J, Li, J, Yuan, Z *et al.* (2009). Hydrodynamic limb vein injection of adeno-associated virus serotype 8 vector carrying canine myostatin propeptide gene into normal dogs enhances muscle growth. *Hum Gene Ther* **20**: 1–10.
128. Morine, KJ, Bish, LT, Selsby, JT, Gazzara, JA, Pendrak, K, Sleeper, MM *et al.* (2010). Activin IIB receptor blockade attenuates dystrophic pathology in a mouse model of Duchenne muscular dystrophy. *Muscle Nerve* **42**: 722–730.
129. Kobinger, GP, Louboutin, JP, Barton, ER, Sweeney, HL and Wilson, JM (2003). Correction of the dystrophic phenotype by *in vivo* targeting of muscle progenitor cells. *Hum Gene Ther* **14**: 1441–1449.
130. Kimura, E, Li, S, Gregorevic, P, Fall, BM and Chamberlain, JS (2010). Dystrophin delivery to muscles of *mdx* mice using lentiviral vectors leads to myogenic progenitor targeting and stable gene expression. *Mol Ther* **18**: 206–213.
131. Bachrach, E, Li, S, Perez, AL, Schienda, J, Liadaki, K, Volinski, J *et al.* (2004). Systemic delivery of human microdystrophin to regenerating mouse dystrophic muscle by muscle progenitor cells. *Proc Natl Acad Sci USA* **101**: 3581–3586.
132. Bachrach, E, Perez, AL, Choi, YH, Illigens, BM, Jun, SJ, del Nido, P *et al.* (2006). Muscle engraftment of myogenic progenitor cells following intraarterial transplantation. *Muscle Nerve* **34**: 44–52.
133. Sampaolesi, M, Blot, S, D'Antona, G, Granger, N, Tonlorenzi, R, Innocenzi, A *et al.* (2006). Mesoangioblast stem cells ameliorate muscle function in dystrophic dogs. *Nature* **444**: 574–579.
134. Quenneville, SP, Chapdelaine, P, Skuk, D, Paradis, M, Goulet, M, Rousseau, J *et al.* (2007). Autologous transplantation of muscle precursor cells modified with a lentivirus for muscular dystrophy: human cells and primate models. *Mol Ther* **15**: 431–438.
135. Pichavant, C, Chapdelaine, P, Cerri, DG, Dominique, JC, Quenneville, SP, Skuk, D *et al.* (2010). Expression of dog microdystrophin in mouse and dog muscles by gene therapy. *Mol Ther* **18**: 1002–1009.
136. Benchaouir, R, Meregalli, M, Farini, A, D'Antona, G, Belicchi, M, Goyenvalle, A *et al.* (2007). Restoration of human dystrophin following transplantation of exon-skipping-engineered DMD patient stem cells into dystrophic mice. *Cell Stem Cell* **1**: 646–657.
137. Romero, NB, Braun, S, Benveniste, O, Leturcq, F, Hogrel, JY, Morris, GE *et al.* (2004). Phase I study of dystrophin plasmid-based gene therapy in Duchenne/Becker muscular dystrophy. *Hum Gene Ther* **15**: 1065–1076.
138. Budker, V, Zhang, G, Danko, I, Williams, P and Wolff, J (1998). The efficient expression of intravascularly delivered DNA in rat muscle. *Gene Ther* **5**: 272–276.
139. Hagstrom, JE, Hegge, J, Zhang, G, Noble, M, Budker, V, Lewis, DL *et al.* (2004). A facile nonviral method for delivering genes and siRNAs to skeletal muscle of mammalian limbs. *Mol Ther* **10**: 386–398.
140. Wolff, J, Lewis, DL, Herweijer, H, Hegge, J and Hagstrom, J (2005). Non-viral approaches for gene transfer. *Acta Myol* **24**: 202–208.
141. Hegge, JO, Wooddell, CI, Zhang, G, Hagstrom, JE, Braun, S, Huss, T *et al.* (2010). Evaluation of hydrodynamic limb vein injections in nonhuman primates. *Hum Gene Ther* **21**: 829–842.
142. Zhang, G, Wooddell, CI, Hegge, JO, Griffin, JB, Huss, T, Braun, S *et al.* (2010). Functional efficacy of dystrophin expression from plasmids delivered to *mdx* mice by hydrodynamic limb vein injection. *Hum Gene Ther* **21**: 221–237.
143. Thibaud, JL, Huss, T, Hegge, J, Thioudellet, C, Granger, N, Gnirs, K *et al.* (2006) Intravascular administration of dystrophin plasmid DNA in a canine model of Duchenne muscular dystrophy: early side effects and long-term biological efficacy. *J Vet Intern Med* **20**: 1270.
144. Aihara, H and Miyazaki, J (1998). Gene transfer into muscle by electroporation in vivo. *Nat Biotechnol* **16**: 867–870.
145. Mir, LM, Bureau, MF, Gehl, J, Rangara, R, Rouy, D, Caillaud, JM *et al.* (1999). High-efficiency gene transfer into skeletal muscle mediated by electric pulses. *Proc Natl Acad Sci USA* **96**: 4262–4267.
146. Gissel, H and Clausen, T (2001). Excitation-induced Ca_2+ influx and skeletal muscle cell damage. *Acta Physiol Scand* **171**: 327–334.
147. Trollet, C, Scherman, D and Bigey, P (2008). Delivery of DNA into muscle for treating systemic diseases: advantages and challenges. *Methods Mol Biol* **423**: 199–214.
148. Marshall, WG Jr, Boone, BA, Burgos, JD, Gografe, SI, Baldwin, MK, Danielson, ML *et al.* (2010). Electroporation-mediated delivery of a naked DNA plasmid expressing VEGF to the porcine heart enhances protein expression. *Gene Ther* **17**: 419–423.
149. Peng, B, Zhao, Y, Lu, H, Pang, W and Xu, Y (2005). *In vivo* plasmid DNA electroporation resulted in transfection of satellite cells and lasting transgene expression in regenerated muscle fibers. *Biochem Biophys Res Commun* **338**: 1490–1498.
150. Trollet, C, Bloquel, C, Scherman, D and Bigey, P (2006). Electrotransfer into skeletal muscle for protein expression. *Curr Gene Ther* **6**: 561–578.
151. Mir, LM, Belehradek, M, Domenge, C, Orlowski, S, Poddevin, B, Belehradek, J Jr *et al.* (1991). [Electrochemotherapy, a new antitumor treatment: first clinical trial]. *C R Acad Sci III, Sci Vie* **313**: 613–618.
152. Favard, C, Dean, DS and Rols, MP (2007). Electrotransfer as a non viral method of gene delivery. *Curr Gene Ther* **7**: 67–77.
153. Bodles-Brakhop, AM, Heller, R and Draghia-Akli, R (2009). Electroporation for the delivery of DNA-based vaccines and immunotherapeutics: current clinical developments. *Mol Ther* **17**: 585–592.
154. Mir, LM (2008). Application of electroporation gene therapy: past, current, and future. *Methods Mol Biol* **423**: 3–17.
155. Chapdelaine, P, Moisset, PA, Campeau, P, Asselin, I, Vilquin, JT and Tremblay, JP (2000). Functional EGFP-dystrophin fusion proteins for gene therapy vector development. *Protein Eng* **13**: 611–615.
156. Vilquin, JT, Kennel, PF, Paturneau-Jouas, M, Chapdelaine, P, Boissel, N, Delaère, P *et al.* (2001). Electrotransfer of naked DNA in the skeletal muscles of animal models of muscular dystrophies. *Gene Ther* **8**: 1097–1107.
157. Pichavant, C, Chapdelaine, P, Cerri, DG, Bizario, JC and Tremblay, JP (2010). Electrotransfer of the full-length dog dystrophin into mouse and dystrophic dog muscles. *Hum Gene Ther* **21**: 1591–1601.
158. Zaiss, AK and Muruve, DA (2008). Immunity to adeno-associated virus vectors in animals and humans: a continued challenge. *Gene Ther* **15**: 808–816.
159. Roy, R, Tremblay, JP, Huard, J, Richards, C, Malouin, F and Bouchard, JP (1993). Antibody formation after myoblast transplantation in Duchenne-dystrophic patients, donor HLA compatible. *Transplant Proc* **25**(1 Pt 2): 995–997.

Molecular and Cellular Neuroscience 47 (2011) 119–130

Contents lists available at ScienceDirect

Molecular and Cellular Neuroscience

journal homepage: www.elsevier.com/locate/ymcne

Reactive gliosis of astrocytes and Müller glial cells in retina of POMGnT1-deficient mice

Hisatomo Takahashi [a], Hironori Kanesaki [b,c], Tsutomu Igarashi [d], Shuhei Kameya [a,*], Kunihiko Yamaki [a], Atsushi Mizota [e], Akira Kudo [b], Yuko Miyagoe-Suzuki [c], Shin'ichi Takeda [c], Hiroshi Takahashi [d]

[a] Department of Ophthalmology, Nippon Medical School Chiba Hokusoh Hospital, 1715 Kamagari, Inzai, Chiba 270-1694, Japan
[b] Department of Biological Information, Tokyo Institute of Technology, 4259 Nagatsuta, Midori-ku, Yokohama 226-8501, Japan
[c] Department of Molecular Therapy, National Institute of Neuroscience, National Center of Neurology and Psychiatry, 4-1-1 Ogawahigashi, Kodaira, Tokyo 187-8502, Japan
[d] Department of Ophthalmology, Nippon Medical School, 1-1-5 Sendagi, Bunkyo-ku, Tokyo 113-8602, Japan
[e] Department of Ophthalmology, Teikyo University of Medicine, 2-11-1 Kaga, Itabashi-ku, Tokyo 173-8605, Japan

ARTICLE INFO

Article history:
Received 19 November 2010
Revised 5 March 2011
Accepted 21 March 2011
Available online 8 April 2011

Keywords:
Muscle–eye–brain disease
Dystroglycan
Retinal detachment

ABSTRACT

Protein O-linked mannose beta1, 2-N-acetylglucosaminyltransferase 1 (POMGnT1) is an enzyme that catalyzes the transfer of N-acetylglucosamine to O-mannose of glycoproteins. Alpha-dystroglycan, a substrate of POMGnT1, is concentrated around the blood vessels, in the outer plexiform layer (OPL), and in the inner limiting membrane (ILM) of the retina. Mutations of the *POMGnT1* gene in humans cause muscle-eye-brain (MEB) disease. Several ocular abnormalities including retinal dysplasia, ERG abnormalities, and retinal detachments have been reported in patients with MEB. We have analyzed the eyes of POMGnT1-deficient mice, generated by standard gene targeting technique, to study the retinal abnormalities. Clinical examination of adult mutant mice revealed a high incidence (81% by 12-months-of-age) of retinal detachments. Sheathing of the retinal vessels and the presence of ectopic fibrous tissues around the optic nerve head were also found. Histological examinations showed focal retinal detachment associated with GFAP immunopositivity. The ILM of the mutant mice was disrupted with ectopic cells near the disruptions. The expression of Dp71, a shorter isoform of dystrophin, was severely reduced in the ILM and around retinal blood vessels of POMGnT1-deficient mice. The expression of Dp427, Dp260, Dp140 were also reduced in the OPL of the mutant mice. Electroretinographic (ERG) analyses showed reduced a- and b-wave amplitudes. Examinations of flat mounts revealed abnormal vascular network associated with highly irregular astrocytic processes. In addition, ER-TR7-positive fibrous tissue was found closely associated with reactive astrocytes especially around the optic nerve head. Our results suggest that altered glycosylation of alpha-DG may be responsible for the reactive gliosis and reticular fibrosis in the retina, and the subsequent developments of retinal dysplasia, abnormal ERGs, and retinal detachment in the mutant mice.

Introduction

Protein O-linked mannose beta1, 2-N-acetylglucosaminyltransferase 1 (POMGnT1) is an enzyme that catalyzes the transfer of N-acetylglucosamine to O-mannose of glycoproteins (Yoshida et al., 2001). Mutations of the *POMGnT1* gene cause muscle–eye–brain (MEB) disease, one of a family of dystroglycanopathies, in humans (Yoshida et al., 2001). The dystroglycanopathies include a group of muscular dystrophies including Walker-Warburg syndrome (WWS), Fukuyama-type congenital muscular dystrophy (FCMD), congenital muscular dystrophy (MDC) 1C/D, limb-girdle muscular dystrophy (LGMD) 2I/K/M/N, and MEB. This group of disorders is clinically characterized by various combinations of severe muscular dystrophy, mental retardation, and ocular abnormalities. To date, mutations in six known or putative glycosyltransferase genes, viz., *POMT1*, *POMT2*, *Fukutin*, *FKRP*, *LARGE*, and *POMGnT1*, have been identified to be associated with these disorders (Beltrán-Valero de Bernabé et al., 2002; van Reeuwijk et al., 2005; Kobayashi et al., 1998; Brockington et al., 2001; Longman et al., 2003). A common molecular defect for the dystroglycanopathies is the post-translational modification or hypoglycosylation of alpha-dystroglycan (alpha-DG).

Dystroglycan (DG) is encoded by a single gene and is cleaved into two proteins, alpha-DG and beta-DG, by post-translational processing (Ibraghimov-Beskrovnaya et al., 1992). Alpha-DG is a heavily glycosylated glycoprotein and is a central component of the dystrophin glycoprotein complex (DGC). A major function of the DGC is to link cytoskeletal actin to the basal lamina which maintains the structural integrity of skeletal muscles (Ervasti and Campbell, 1993). Mutations in the components of DGC cause various forms of muscular dystrophies (Straub and Campbell, 1997).

* Corresponding author. Fax: +81 476 99 1923.
E-mail address: shuheik@nms.ac.jp (S. Kameya).

1044-7431/$ – see front matter © 2011 Elsevier Inc. All rights reserved.
doi:10.1016/j.mcn.2011.03.006

DG and other components of DGC are widely expressed in the CNS and the retina (Henry and Campbell, 1999; Blake and Kröger, 2000). Alpha-DG functions as a cell surface receptor for laminin, perlecan, agrin, neurexin, and pikachurin in a variety of tissues (Ervasti and Campbell, 1993; Gee et al., 1994; Peng et al., 1998; Sugita et al., 2001; Sato et al., 2008).

In the retina, alpha-DG is concentrated in the inner limiting membrane (ILM), around blood vessels, and in the outer plexiform layer (OPL; Blake and Kröger, 2000). The alpha-DG in the ILM is concentrated at the endfeet of the Müller cells, and that in the blood vessels in the perivasular astrocytes (Montanaro et al., 1995; Claudepierre et al., 1999). The alpha-DG in the OPL is localized around the site of expression of ribbon synapses of rod and cone photoreceptor terminals (Ueda et al., 1995; Montanaro et al., 1995).

Abnormal electroretinograms (ERGs) have been recorded from patients with MEB disease (Pihko et al., 1995; Fahnehjelm et al., 2001), and have frequently been recorded from individuals with Duchenne and Becker muscular dystrophies (Pillers et al., 1999). The findings in several mouse models with disruption of dystrophin, *Large*^{vls} and fukutin indicated that DGC is associated with the normal physiology of the retina (Pillers et al., 1995; Kameya et al., 1997; Lee et al., 2005; Takeda et al., 2003). Abnormal ERGs in mice with a targeted disruption of pikachurin, an extracellular ligand of alpha-dystroglycan at ribbon synapses, also support the idea that DGC must be present in the OPL for normal retinal physiology (Sato et al., 2008).

It was recently shown that inactivation of glial specific dystroglycan, located in the endfeet of Müller cells and perivascular astrocytes, led to a reduction of the b-wave of the ERG. This suggested that glial specific dystroglycan also plays an important role in the normal physiology of the retina (Satz et al., 2009).

Patients with MEB have a variety of ocular abnormalities including myopia, glaucoma, anterior chamber malformation, microphthalmia, buphthalmus, nystagmus, strabismus, cataract, chorioretinal atrophy, retinal dysplasia, and retinal detachment (Cormand et al., 2001; Mercuri et al., 2009). The purpose of this study was to determine the effect of altered glycosylation of alpha-DG caused by inactivation of POMGnT1 in the retina. To accomplish this, we studied mice with targeted disruption of the *POMGnT1* gene. We shall show that POMGnT1-deficient mice have a high incidence of retinal detachment with reactive gliosis of the Müller glial cells and the perivascular astrocytes. Our results suggest that altered glycosylation of alpha-DG may be responsible for the retinal dysplasia, abnormal ERGs, and retinal detachment in humans with MEB.

Results

Retinal detachment in POMGnT1-deficient mice

At 6-weeks-of-age, the retinal vessels of all POMGnT1-deficient mice were tortuous but none of the mice had a retinal detachment (Fig. 1B). These mutant mice also had fibrous tissue over the retina especially around the optic nerve head (Fig. 1B). Fibrous tissues were not observed in any of the wild type mice.

By 6-months-of-age, the retinal vessels were sheathed, and focal and extensive retinal detachments were present in the areas of the sheathed vessels (Fig. 1C). The retinal detachment of some of the mice covered

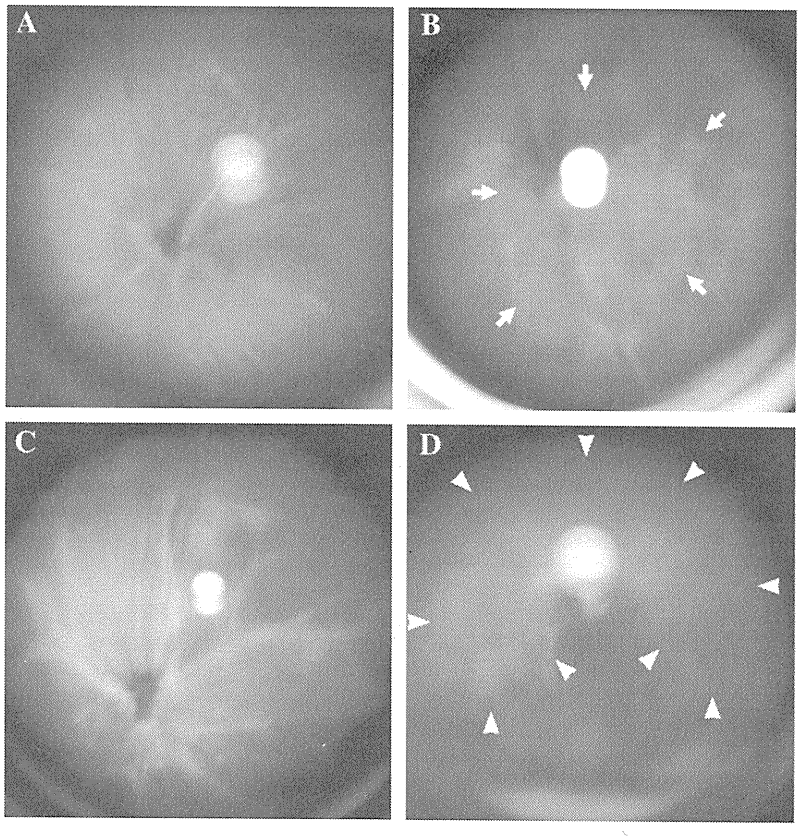

Fig. 1. Fundus photograph of wild-type and POMGnT1-deficient mice. A. Six-week-old wild type mouse. B. Retinal vessel tortuosity can be seen in this 6-week-old POMGnT1-deficient mouse. Arrows point to ectopic fibrous tissue surrounding the optic nerve head. C. Six-month-old POMGnT1-deficient mouse showing sheathing of the retinal vessels. D. Retinal detachment (arrowheads) in a 6-month-old POMGnT1-deficient mouse.

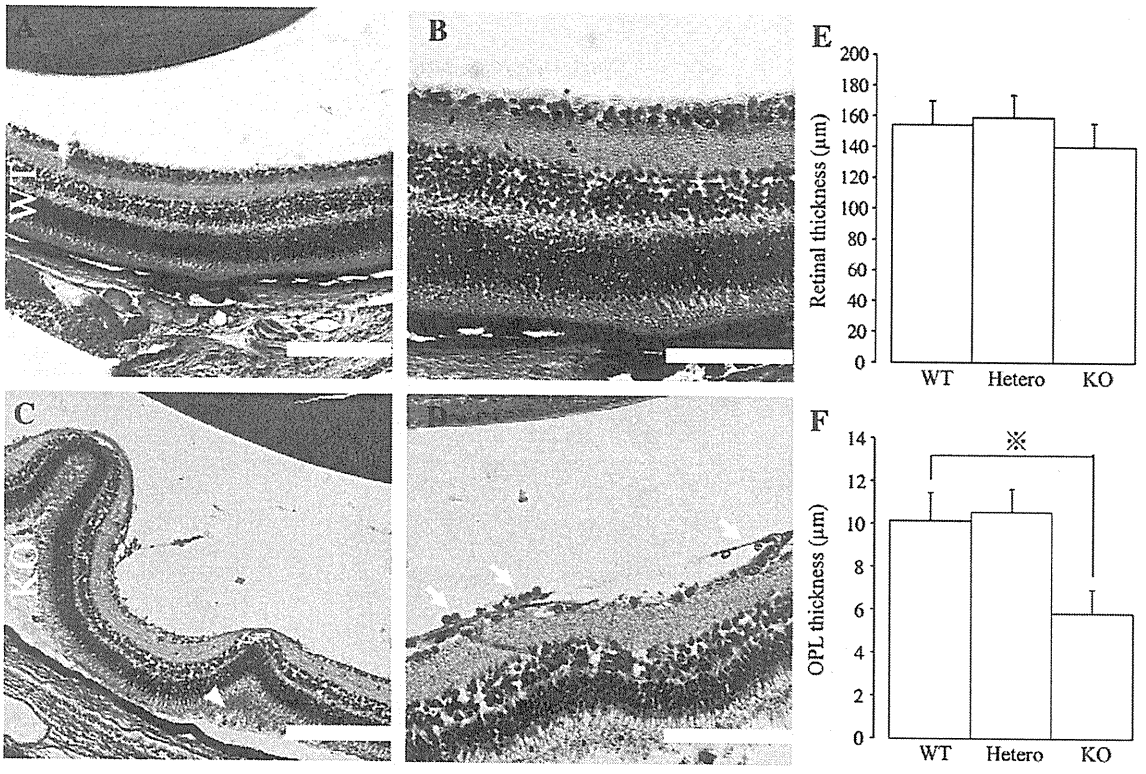

Fig. 2. Histological observations of the retina of wild-type and POMGnT1-deficient mice. A. and B. Sections of 15-week-old wild-type retinas stained with hematoxylin and eosin. C. and D. Sections of 15-week-old POMGnT1-deficient retinas stained with hematoxylin and eosin. In (C), focal retinal detachments can be seen in several regions. There are some connective tissue-like materials beneath the detached retina (arrowhead), indicating the retinal detachments are not embedding or sectioning artifacts. In (D), ectopic cells and vitreal fibroplasia can be seen on the ILM of POMGnT1-deficient retina (arrows). Scale bars represent 200 μm in A, C and 100 μm in B, D E and F. Quantification of the retinal thickness-measurements of wild-type, Heterozygous and Homozygous POMGnT1-deficient mice. Animals used for this study ranged from 18-week-old to 28-week-old. The average of each 5 animals is plotted. There was no significant difference in the whole retinal thickness (E), but significant thinning of the OPL was observed in POMGnT1-deficient mice compared to wild-type mice (10.12 ± 1.34 μm [SD] vs. 5.84 ± 1.13 μm; P = 0.045) (F).

more than a quadrant of the retina (Fig. 1D). By 12-months-of-age, 13 of 16 mutant eyes (81%) showed obvious retinal detachments.

Histological examination of 15-week-old mutant mice showed focal retinal detachments (Fig. 2C). Ectopic cells and vitreal fibroplasia were found on the inner limiting membrane (ILM; Fig. 2D) as was found in Large^{vls} mice (Lee et al., 2005). There were no significant difference in the whole retinal thickness, but significant thinning of the OPL was observed in POMGnT1-deficient mice compared to wild-type mice (Figs. 2E and F). This fibroplasia was immunopositive for glial fibrillary acidic protein (GFAP; Figs. 3C and D). Because GFAP expression is a reliable early marker of reactive gliosis of the astrocytes and Müller glial cells (Lewis and Fisher, 2003), an up-regulation of GFAP staining of the ILM and the radial immunoreactivity in the mutant mice indicated the development of reactive gliosis of the Müller cells. Quantitative analysis revealed that GFAP immunoreactivity was significantly elevated in the retina of POMGnT1-deficient mice (Fig. 3E). To confirm if elevated immunoreactivity of GFAP is truly associated with gliosis, we have also characterized the retina of POMGnT1-deficient mice using anti-vimentin antibody that is other cellular marker associated with gliosis. The vimentin immunoreactivity of POMGnT1-deficient mice along with ILM and radial morphology of Müller cells are also upregulated compared to that of wild-type mice (Figs. 4A and B). We have applied another cellular markers to characterize the different cell types in the anatomical regions. Immunoreactivity for both anti-syntaxin antibody and anti-PKC antibody, cellular markers for amacrine cells and bipolar cells, revealed no obvious differences between POMGnT1-deficient and wild-type mice (Figs. 4C–F). These data indicate that the up-regulation of GFAP and vimentin immunoreactivity is specifically associated with gliosis of Müller cells of the POMGnT1-deficient mice in the region.

Electroretinographic findings of POMGnT1-deficient mice

To examine the function of the retina of POMGnT1-deficient mice, ERGs were recorded from 4-month-old wild type and POMGnT1-deficient mice. The mixed rod–cone ERGs recorded from POMGnT1-deficient mice at higher stimulus intensities had a negative waveform with the amplitude of the b-wave smaller than that of the a-wave (Fig. 5A). Amplitudes of the a-wave and b-wave of mixed rod–cone ERGs obtained from POMGnT1-deficient mice are reduced significantly compared to wild-type mice (Figs. 5B and C). The amplitudes of the scotopic b-wave elicited by lower stimulus intensities were also reduced in POMGnT1-deficient mice (Fig. 5D). The amplitude of the b-wave of photopic ERGs of POMGnT1-deficient mice was also reduced and significantly smaller than that of wild-type mice (Fig. 5E).

Expression of alpha-DG and dystrophin in retina of POMGnT1-deficient mice

To confirm that the retina of POMGnT1-deficient mice completely lacked POMGnT1 enzyme activity, we used a monoclonal antibody, VIA4-1, that reacts against the sugar moiety of alpha-DG. Our findings showed that VIA4-1 immunoreactivity was present on the ILM, around blood vessels, and in the OPL of the retina of the wild type mice but was completely absent in the POMGnT1-deficient mice (Figs. 6A and B). It has been clearly shown that at the OPL there are three DMD gene products, Dp427 (or full length dystrophin), Dp260 and Dp140 and at

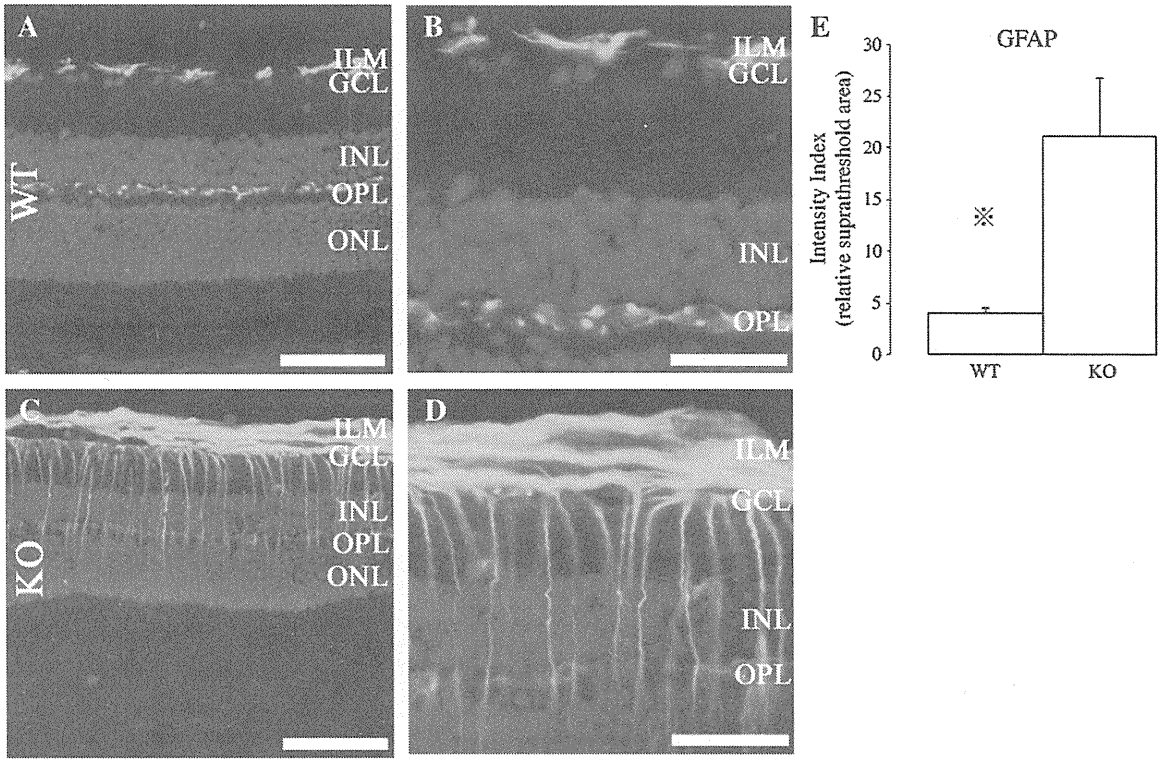

Fig. 3. GFAP staining of paraffin sections from wild-type and POMGnT1-deficient mice. A. and B. Sections of 18-week-old wild-type retinas with GFAP staining. C. and D. Sections of 18-week-old POMGnT1-deficient retinas. There was an up-regulation of GFAP staining in the ILM. Scale bars represent 100 μm in A, C and 50 μm in B, D and E. Quantification of GFAP immunoreactivity in paraffin sections from wild-type and POMGnT1-deficient mice. Animals used for this study ranged from 18-week-old to 28-week-old. The average of each 3 animals is plotted. Intensity Index for GFAP immunoreactivity was significantly elevated in the retina of POMGnT1-deficient mice compared to wild-type mice (3.90 ± 0.54 [SD] vs. 20.61 ± 5.65; P = 0.003).

the Müller cells only Dp71 is found (Dalloz et al., 2003 and Fort et al., 2008). The expression of Dp71 in the ILM and around retinal blood vessels of POMGnT1-deficient mice was severely reduced (Fig. 6D). The expression of Dp427, Dp260, Dp140 were also reduced in the OPL of the mutant mice (Fig. 6D).

Glial proliferation closely associated with ER-TR7-positive fibrous tissue around abnormal retinal vessels in POMGnT1-deficient mice

Two mouse models with aberrant glycosylation of alpha-DG have been reported to have reactive gliosis with an up-regulation of GFAP expression in the retina and the brain. One of these is the *Large*^{vls} mice, which has a disorganization of astrocytic processes in the retina (Lee et al., 2005). The second mutant is the POMGnT1-disrupted mouse, which has reactive gliosis in the cerebral cortex (Yang et al., 2007). To further characterize the glial proliferation and associated vascular abnormalities in the retina of our POMGnT1-deficient mice, we examined flat mounts of the retina of 4-month-old wild type and POMGnT1-deficient mice.

In flat mounts of POMGnT1-deficient mice retina, the GFAP staining of astrocytes was highly irregular especially around the retinal vasculature (Figs. 7E and K). Retinal vascular staining derived from perfusion of FITC-dextran showed disorganization of the normal pattern of the vascular networks (Figs. 7D and J). Double staining for GFAP and FITC-dextran showed that abnormal retinal vasculature was highly co-localized with the irregular astrocytic processes (Figs. 7F and L). Quantitative analysis for GFAP immunoreactivity and vascularization stained by FITC dextran perfusion showed significant elevation of intensity index in both central and peripheral retina of POMGnT1-deficient mice compared to wild-type mice (Fig. 8).

In POMGnT1-deficient mice, it was also reported that most of the GFAP-positive reactive astrocytes in the brain were in close contact with ectopic fibroblasts, suggesting that they were induced by the fibroblasts (Yang et al., 2007). To confirm that our POMGnT1-deficient mice also showed fibrosis associated with the GFAP-positive reactive astrocytes in the retina, we examined flat mounts of 4-month-old wild type and POMGnT1-deficient mice using the ER-TR7 antibody. Although the antigen of the ER-TR7 antibody has not been fully characterized, it is known to detect an antigen present in and produced by reticular fibroblasts. Reticular fibers are synthesized by a family of collagen proteins, and the fibers are made by reticular fibroblasts.

In the flat mount preparations, ER-TR7-positive fibrous tissue was found closely associated with GFAP-positive reactive astrocytes especially around the optic nerve head (Figs. 9D–F). An up-regulation of ER-TR7-positive fibrous tissue was also found in the peripheral retina associated with the irregular retinal vasculature (Figs. 9J–L).

Discussion

Patients with MEB show a variety of ocular abnormalities, and at least six cases with retinal detachment have been reported (Cormand et al., 2001; Matsumoto et al., 2005; Godfrey et al., 2007; Demir et al., 2009). Although an involvement of the retina has been frequently described in MEB patients, many patients without any retinal abnormalities have also been reported (Mercuri et al., 2009). A broader phenotypic spectrum was reported for MEB disease worldwide, and no consistent genotype–phenotype correlation has been established (Hehr et al., 2007). Thus, Finnish patients homozygous for the founder mutation showed a wide variation in their phenotype (Diesen et al., 2004).

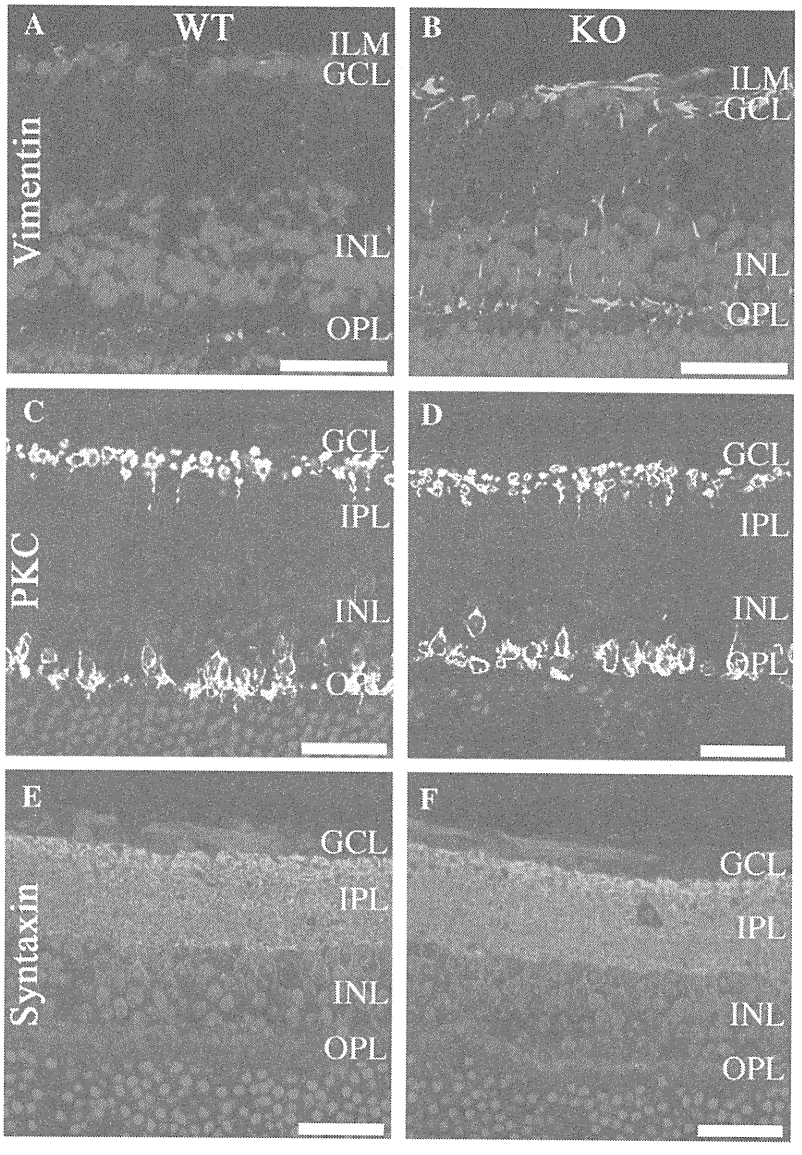

Fig. 4. Immunohistochemical observations of several markers for different cell types of the regions from 18-week-old wild-type and 20-week-old POMGnT1-deficient mice. A. and B. Sections of retina labeled with anti-vimentin antibody. The vimentin immunoreactivity of POMGnT1-deficient mice along with ILM and radial morphology of Müller cells were upregulated compared to that of wild-type mice. C. and D. Sections of retina labeled with anti-PKC antibody for bipolar cells. There were no significant differences between the retina of wild-type and POMGnT1-deficient mice. E. and F. Sections of retina labeled with anti-Syntaxin antibody for amacrine cells. There were no significant differences between the retina of wild-type and POMGnT1-deficient mice. Scale bars represent 50 μm in A–F.

Two mouse models with mutations of the *POMGnT1* gene have been reported including our model (Liu et al., 2006 and Hu et al., 2010; Miyagoe-Suzuki et al., 2009). These two mouse models have different phenotypes and different location of the POMGnT1 gene mutation. Our model was produced by standard gene targeting techniques with disruption of exon 18, while the other model was generated by gene trapping with a retroviral vector inserted into exon 2 of the *POMGnT1* gene. Our model has a milder muscle phenotype and a lower survival rate than the other model, but had frequent retinal detachment which was not described in the other model. Homozygous mutants of our mouse model are sterile, and homozygous mutants are obtained by heterozygote matings. However, the homozygous offsprings have a very low survival rate (Miyagoe-Suzuki et al., 2009).

A spectrum of retinal abnormalities was observed in our POMGnT1-deficient mice, although all of these mice had the same *POMGnT1* gene mutation. These findings are consistent with earlier hypotheses that factors other than the activity of *POMGnT1* gene, e.g., environmental factors, play a role in determining the severity of the mutation (Diesen et al., 2004; Matsumoto et al., 2005).

Abnormal ERGs are found in patients and mice with a mutation in the DGC component (Pillers et al., 1993; Pihko et al., 1995; Kameya et al., 1997). These findings suggest an involvement of the DGC localized in the OPL for signal transduction at the ribbon synapse of photoreceptor terminals. Mice with targeted disruption with pikachurin gene support this hypothesis. The reduced ERG b-waves in pikachurin-deficient mice suggest an involvement of DGC and pikachurin in retinal signal transduction at the ribbon synapses of photoreceptors (Sato et al., 2008). Recently, mice with a conditional deletion of dystroglycan in the CNS were generated by Satz et al. These mice showed that an inactivation of the glial specific dystroglycan located in the glial endfeet of Müller cells and perivascular astrocytes was sufficient to reduce the amplitude of the ERG b-wave (Satz et al., 2009).

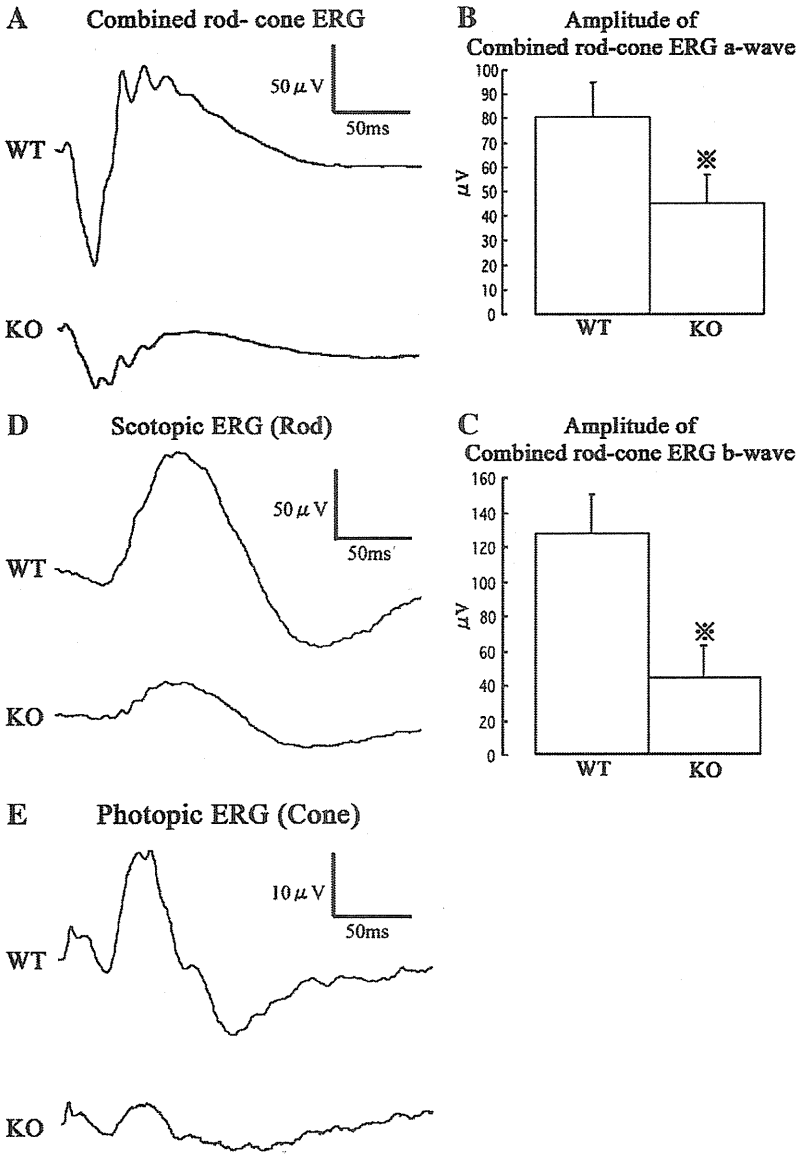

Fig. 5. Electroretinograms of wild-type and POMGnT1-deficient mice. Animals used for this study ranged from 11-week-old to 19-week-old. A. Combined rod–cone ERGs obtained from POMGnT1-deficient mouse showing negative-type ERG with decreased amplitude of a-wave and b-wave. B. and C. Amplitudes of the a-wave and b-wave of combined rod–cone ERGs obtained from POMGnT1-deficient mice are reduced significantly compared to wild-type mice. The average of each 3 animals is plotted. D. and E. Amplitudes of the b-wave of scotopic and photopic ERGs obtained from POMGnT1-deficient mice are also decreased compared to wild-type mice.

The abnormal ERGs of POMGnT1-deficient mice could be explained by several mechanisms. They could arise from an inactivation of glial specific alpha-DG, or disturbed Pikachurin-DG interaction at the ribbon synapse, or dysfunction of retina caused by vascular network abnormalities, or the retinal detachments.

POMGnT1-deficient mice showed decreased expression of dystrophin in the ILM similar to that observed in the mice with conditional deletion of dystroglycan in the CNS, suggesting inactivation or dysfunction of alpha-DG caused by hypogycosylation.

Pikachurin is necessary for the apposition of presynaptic and postsynaptic terminals in the photoreceptor ribbon synapses because Pikachurin is an extracellular ligand of alpha-dystroglycan at ribbon synapses (Sato et al., 2008). A recent study using the same POMGnT1-deficient model clearly showed that the degree of pikachurin immnoreactivity in the ribbon synapse of the mutant mice is reduced (Kanagawa et al., 2010). Because a proper localization of pikachurin at the ribbon synapse supported by functionally mature DG plays important roles in the physiology of the retina, reduced expression of pikachurin in the mutant mice caused by disturbed pikacurin-DG interaction could be one of the cause of abnormal ERG of POMGnT1-deficient mice.

The vascular networks in the mutant retina were grossly disorganized associated with GFAP-positive irregular astrocytic processes compared to that of wild-type mice. The dysfunction of the mutant retina caused by the disorganization of retinal vascular network might be one of the causes of abnormal ERGs of mutant mice.

We have obtained the ERG data from the mice without gross retinal detachment, because retinal detachment is generally known to cause abnormal ERGs. However, we cannot rule out the possibility that these mice had shallow and focal retinal detachment associated with sheathed retinal vessels caused by the reactive gliosis.

In the retina, reactive gliosis can result from retinal injury and disease, including retinal trauma, choroidal neovascularization, retinal detachment, and diabetic retinopathy (MacLaren, 1996; Caicedo et al.,

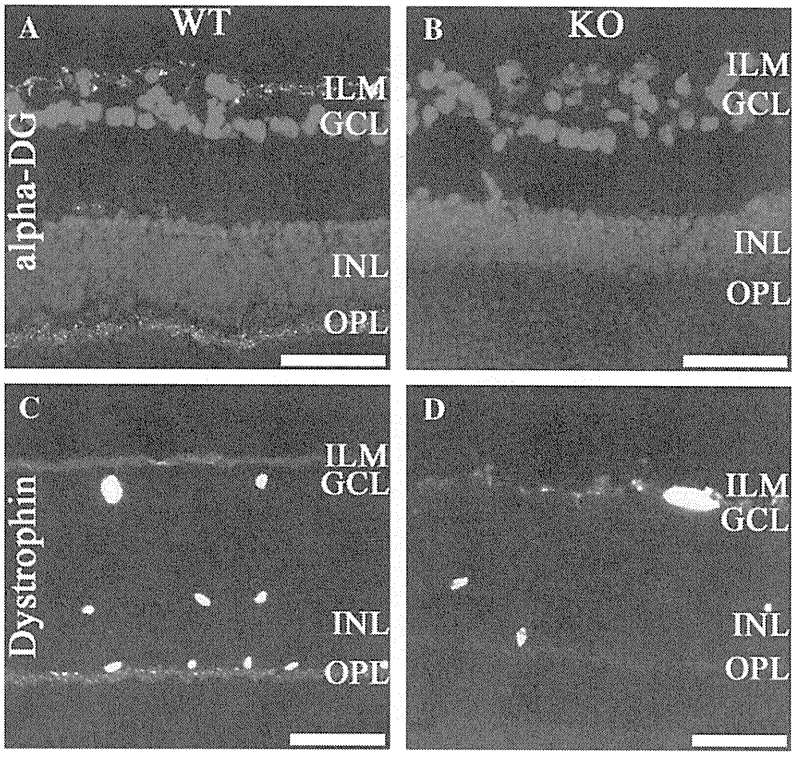

Fig. 6. Immunohistochemical observations of the dystrophin–glycoprotein complex in the retina from 18-week-old wild-type and 20-week-old POMGnT1-deficient mice. A. Sections of wild-type retina labeled with the VIA4-1 antibody for alpha-dystroglycan. VIA4-1 staining was found in ILM, around blood vessels, and in the OPL. B. VIA4-1 immunoreactivity was completely absent in POMGnT1-deficient retina. C. Sections of wild-type retinas labeled with the MAB1694 antibody for Dystrophin. Expression of Dystrophin can be seen in ILM, around blood vessels, and in the OPL. D. In the retina of POMGnT1-deficient mice, expression of Dystrophin was reduced in ILM, around the blood vessels and OPL. Scale bars represent 50 μm in A–D.

2005; Lewis et al., 1995; Mizutani et al., 1998). Secondary complications induced by the reactive gliosis of the Müller cells and astrocytes are the development of fibrosis and proliferative vitreoretinopathy (PVR; Fisher and Lewis, 2003). The POMGnT1-deficient mice showed highly reactive gliosis with strong up-regulation of GFAP expression.

Flat mount preparations of the mutant mice also showed connective tissue-like ER-TR7-positive fibrosis. The high incidence of retinal detachments in POMGnT1-deficient mice may be caused by the PVR preceding the reactive gliosis and reticular fibrosis in the perivascular astrocytes and Müller cells. In POMGnT1-deficient mice, it was shown that repetitive injury caused more fibrosis and fatty infiltration in the tibiaris anterior muscles (Miyagoe-Suzuki et al., 2009). Reactive gliosis with increased numbers of fibroblasts closely associated with capillaries in the cerebral cortex has been reported in POMGnT1-deficient mice (Yang et al., 2007). *Large*^{vls} mice with disruption of glycosyltransferase have abnormal retinal vessels with highly irregular GFAP staining similar to those observed in our mice (Lee et al., 2005). Our mutant mice also had ER-TR7-positive fibrosis associated with reactive astrocytes around both the optic nerve head and peripheral retina. These findings suggest that aberrant glycosylation of alpha-DG can cause fibroblast proliferation in the muscle, eye, and brain of these mice, and also reactive gliosis in the eye and brain.

On the other hand, mice with a complete loss of dystroglycan from the glial endfeet did not have abnormal retinal vasculature or gliosis (Satz et al., 2009). These results suggest that hypoglycosylation or incomplete glycosylation of alpha-DG rather than the absence of alpha-DG may play a role in reactive gliosis of perivascular astrocytes in the retina.

In conclusion, our findings indicate that POMGnT1-deficient mice may be a good model of human MEB. The reactive gliosis and reticular fibrosis in the perivascular astrocytes and Müller glial cells caused by hypoglycosylation or incomplete glycosylation of alpha-DG may be associated with the mechanisms of retinal dysplasia, abnormal ERG and retinal detachment in human MEB. The phenotypic variability of the mutant mice may be useful to determine other factors than POMGnT1-deficiency in determining the severity of human MEB.

Experimental methods

Experimental animals

The generation of POMGnT1-deficient mice on C57BL/6 background was described in detail by Miyagoe-Suzuki et al. (2009). For our study, normal C57BL/6J mice were used as wild type control and were purchased from CLEA Japan, Inc. The procedures used in these experiments were approved by the Animal Care and Use Committee of the Nippon Medical School and conformed to the ARVO statement for the use of animals in ophthalmic and vision research.

Clinical examination of retina

The pupils of the mice were dilated with tropicamide and phenylephrine hydrochloride for indirect ophthalmoscopy with a 90 diopter aspheric lens. Fundus photographs were taken with a Kowa GENESIS-D fundus camera (Kowa Co., Japan) for small animals using a 90 diopter aspheric lens.

Histology and immunohistochemistry

Eyes from POMGnT1-deficient and C57BL/6J mice were enucleated and fixed in SuperFix (Kurabo, Osaka, Japan) overnight. They were then embedded in paraffin, and 7 μm thickness sections were stained

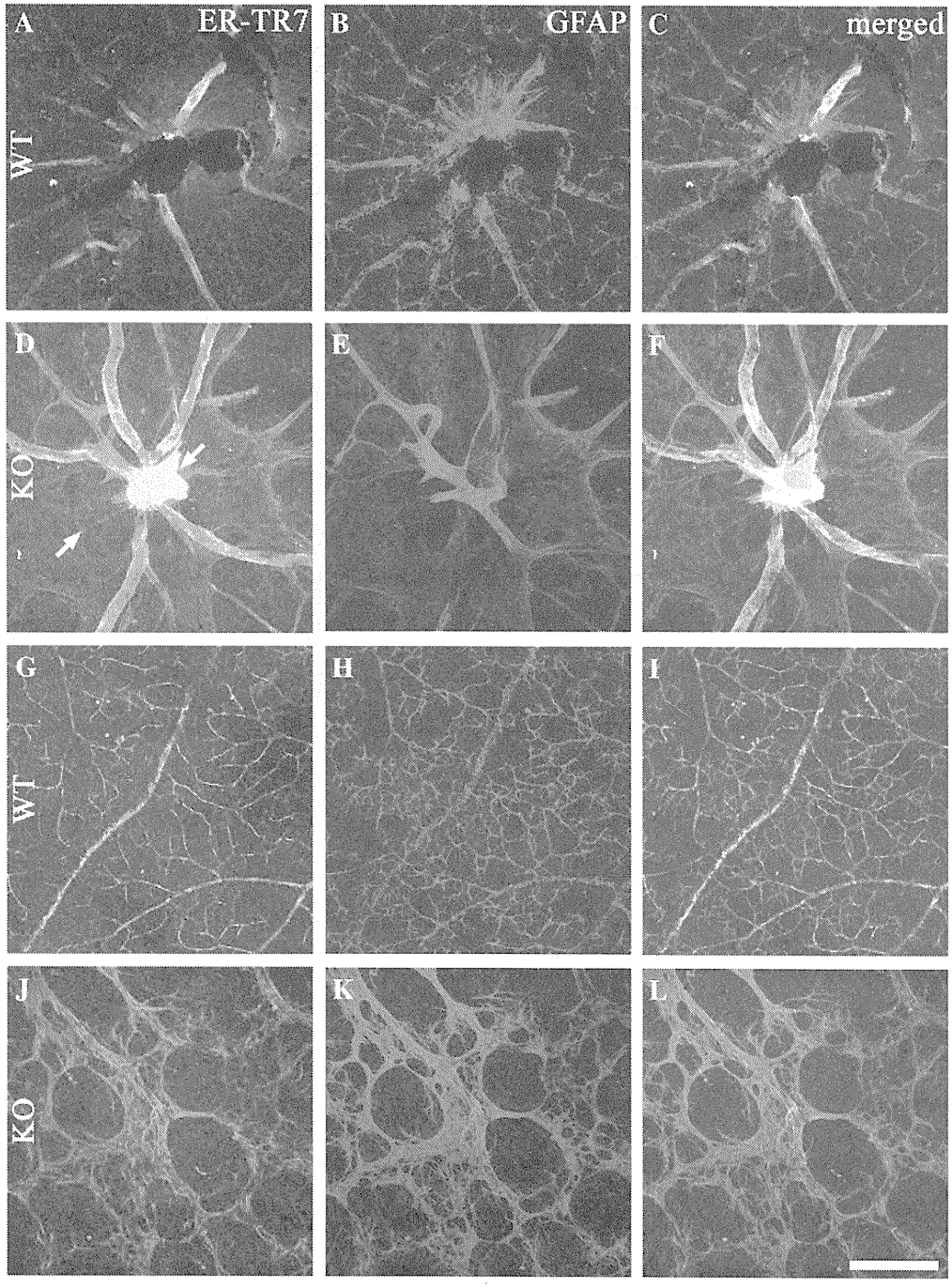

Fig. 7. Vascular network of flat mounted retinas stained by FITC-dextran perfusion and immunohistochemical staining for GFAP from wild-type and POMGnT1-deficient mice. Each animals are 10-week-old. A. D. G. and J. Flat mount retinal preparations from wild-type and POMGnT1-deficient mice perfused with FITC-dextran. B. E. H. and K. GFAP staining of astrocytes in flat mount retinal preparations from wild-type and POMGnT1-deficient mice. C. F. I. and L. Merged images are shown. Regions of central retinas (A–F) and peripheral retinas (G–L) are shown respectively. GFAP staining of astrocytes in POMGnT1-deficient retina is highly irregular especially around retinal vasculature (Eand K). Retinal vascular staining derived from perfusion of FITC-dextran showed disorganization of normal pattern of vascular network (D and J). Double staining of GFAP and FITC-dextran showed that abnormal retinal vasculature was associated with highly irregular astrocytic processes (F and L). Scale bars represent 100 μm in A–L.

with hematoxylin and eosin (H&E). For statistical analysis, measurements of retinal thickness were made at peripheral retina ~1.0–1.2 mm from the optic nerve head (Chi et al., 2010). For immunohistochemical analyses, the enucleated eyes were embedded in optimal cutting temperature compound (OCT, Miles Inc.) and frozen in liquid nitrogen before 6 μm sections were cut. After blocking the sections with 5% normal goat serum, sections were incubated overnight with rabbit polyclonal anti-glial fibrillary acidic protein (GFAP; Dako), anti-vimentin antibody (V9; Dako), anti-PKC antibody (MC5; Sigma), anti-Syntaxin antibody (HPC-1; Sigma), anti-alpha-dystroglycan antibody (VIA4-1; Upstate Biotechnology), or anti-dystrophin antibody (Dys2; Novocastra). The secondary antibodies were anti-mouse antibody conjugated with Alexa Fluor 488 (Molecular Probes) for vimentin, Syntaxin, alpha-dystroglycan, dystrophin, and anti-rabbit antibody

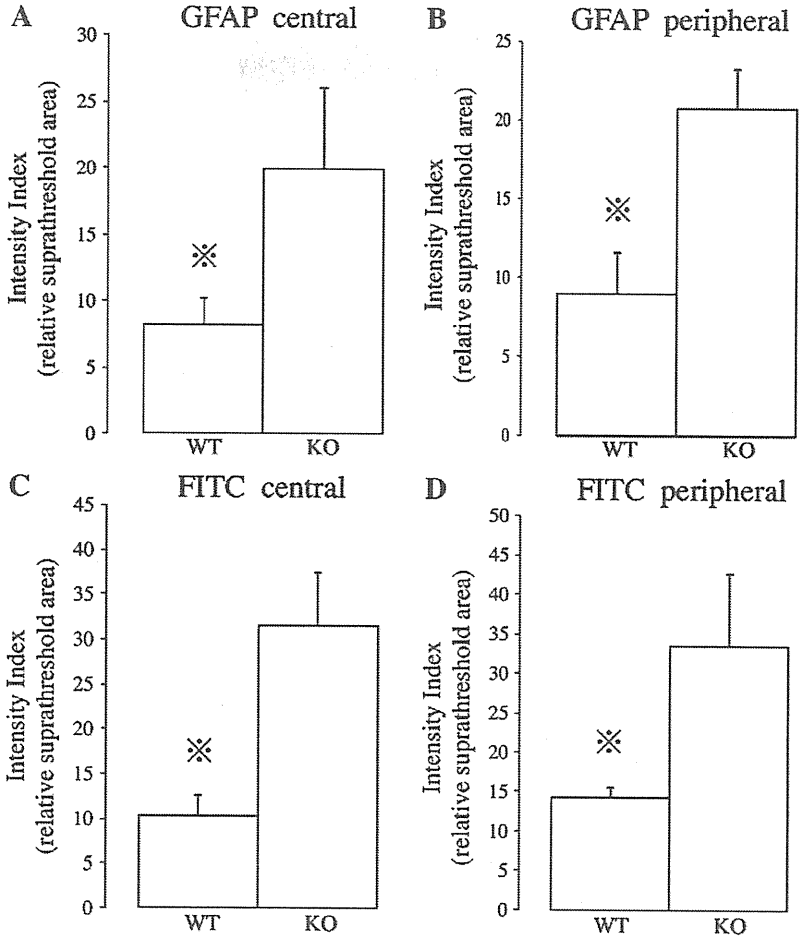

Fig. 8. Quantification of GFAP immunoreactivity and vascularization stained by FITC-dextran perfusion in flat mounted retinas from wild-type and POMGnT1-deficient mice. Animals used for this study ranged from 10-week-old to 12-week-old. The average of each 3 animals is plotted. A. and B. Intensity Index for GFAP immunoreactivity was significantly elevated in the central retina of POMGnT1-deficient mice compared to wild-type mice (8.33 ± 2.00 [SD] vs. 20.23 ± 6.22; $P = 0.003$) (A) and also in the peripheral retina of POMGnT1-deficient mice compared to wild-type mice (9.02 ± 2.54 [SD] vs. 20.70 ± 2.55; $P = 0.005$) (B). C. and D. Intensity Index for vascularization stained by FITC-dextran perfusion was significantly elevated in the central retina of POMGnT1-deficient mice compared to wild-type mice (10.50 ± 2.39 [SD] vs. 32.18 ± 6.04; $P = 0.004$) (C) and also in the peripheral retina of POMGnT1-deficient mice compared to wild-type mice (14.60 ± 1.35 [SD] vs. 34.29 ± 9.30; $P = 0.002$) (D).

conjugated with Alexa Fluor 488 (Molecular Probes) for GFAP, PKC. The immunostained sections were photographed with a confocal laser scanning microscope (TCSSP™, Leica Microsystems Japan).

Electroretinograms (ERGs)

ERGs were recorded from mice anesthesized with an intramuscular injection of ketamine (80 mg/kg) and xylazine (10 mg/kg), and the pupils were dilated with a mixture of tropicamide and phenylephrine. After overnight dark adaptation (>12 h), white light-emitting diodes embedded contact lens electrode was placed on the cornea under dim red light, this electrode was translucent to diffuse the stimulus and background lights. The stimulus intensity and duration were controlled by an electronic stimulator (LS-W; Mayo Co., Nagoya, Japan). The indifferent electrode was a needle inserted subcutaneously on the nasal bone, and a needle electrode on the neck served as the ground electrode. During recording, body temperature was kept to 33 °C with small animals heat controller (ATC-101B, Unique Medical, Tokyo, Japan).

Responses were amplified by a preamplifier (MEG-5200, Nihon Koden, Tokyo, Japan) with band pass between 1 and 300 Hz, and eight responses were recorded with the Power Lab system (AD Instruments Japan Inc., Nagoya, Japan). Stimulus intensity was calibrated by photo sensor built in LS-W. The stimulus intensity to elicit scotopic ERGs was 0.009 cds/m^2, and that to elicit the mixed rod–cone ERGs was 3.0 cds/m^2. Photopic ERGs were recorded after 10 min of light adaptation with 31.6 cd/m^2 and the photopic ERGs were elicited with a stimulus intensity of 3.0 cds/m^2. The interstimulus interval was 10 s for scotopic ERGs, 15 s for combined rod–cone ERGs, and 2 s for the photopic ERGs.

Retinal flat mounts

Anesthetized mice were perfused with 40 ml of PBS through the heart followed by 5 ml of 4% paraformaldehyde in PBS. Then, 2 ml of a mixture of fluorescein-isothiocyanate (FITC)-conjugated high-molecular-weight dextran (molecular weights: 2×10^6 and 4×10^4 Da in a proportion of 2:1 and a concentration of 10 mg/ml; Sigma, St. Louis, MO) was perfused through the heart. The eyes were enucleated and placed in 4% paraformaldehyde overnight at 4 °C. The anterior segment was removed, and four radial incisions were made in the remaining sclera-choroid-neurosensory retina complex. The isolated retinas were placed in ice-cold methanol for 15 min and transferred to PBS. After two 15 min washes in PBS at room temperature (RT), the retinas were transferred into a blocking solution of 10% fetal bovine serum (FBS) and 10% normal goat serum (NGS) for 1 h at RT. The retinas were incubated with rabbit polyclonal anti-glial fibrillary acidic protein (GFAP; Dako) or reticular fibroblasts and reticular fibers antibody (ER-TR7; Santa Cruz

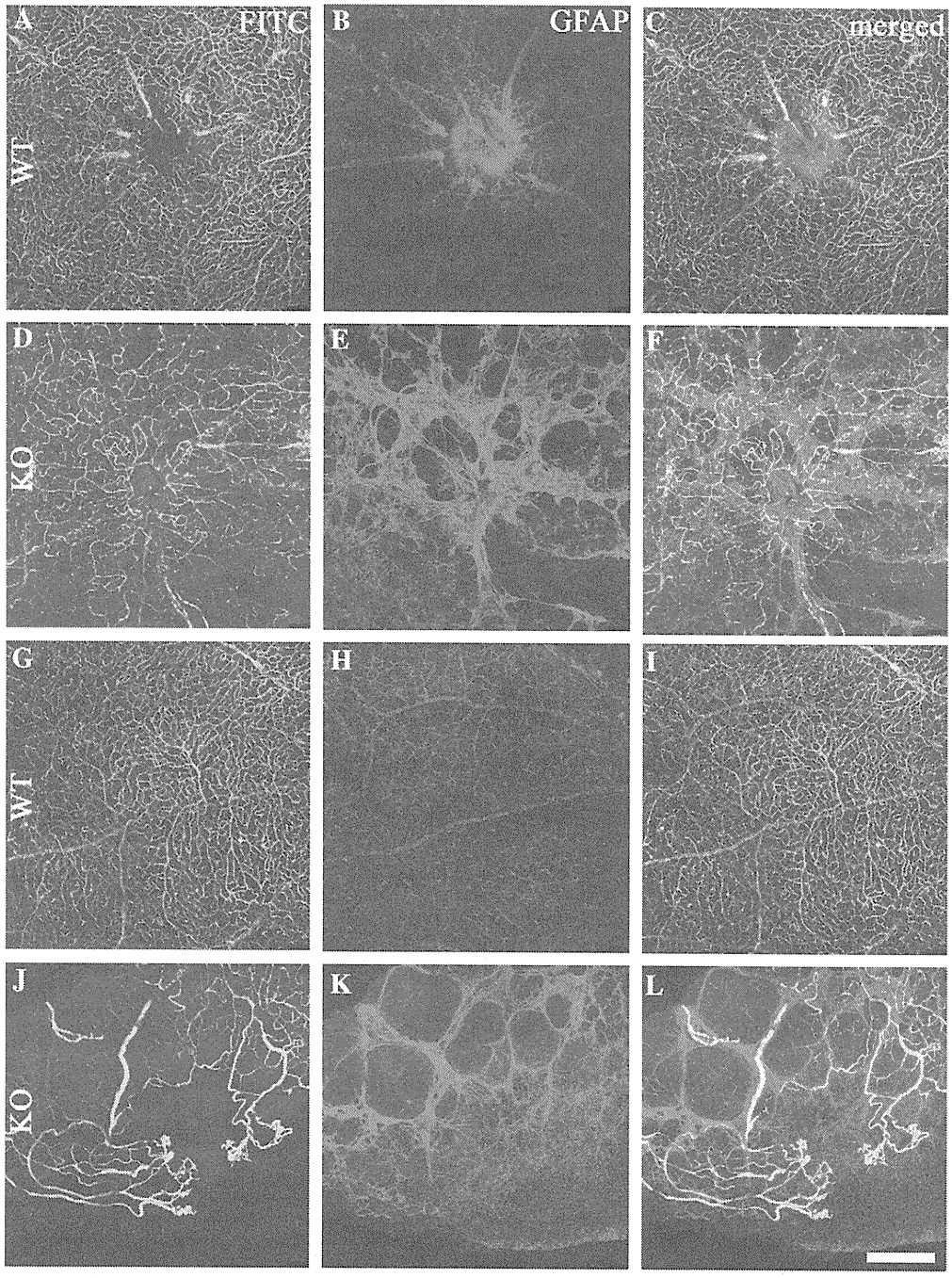

Fig. 9. Immunohistochemical staining for ER-TR7 antigen and GFAP in flat mount retinal preparations from wild-type and POMGnT1-deficient mice. Each animals are 10-week-old. A. D. G. and J. ER-TR7 staining in flat mount retinal preparations from wild-type and POMGnT1-deficient mice. B. E. H. and K. GFAP staining of astrocytes in flat mount retinal preparations from wild-type and POMGnT1-deficient mice. C. F. I. and L. Merged images are shown. Regions of central retinas (A–F) and peripheral retinas (G–L) are shown respectively. ER-TR7-positive fibrous tissues were found closely associated with reactive astrocytes around optic nerve head (D) and peripheral vasculature (J). Note that ER-TR7 and GFAP staining are not identical (arrows). Scale bars represent 100 μm in A–L.

Biotechnology) in 10% FBS and 10% NGS in PBS for 18 h at 4 °C. Retinas were incubated with anti-rabbit antibody conjugated with Alexa Fluor 568 (Molecular Probes) for GFAP, and anti-rat antibody conjugated with Alexa Fluor 488 (Molecular Probes) for ER-TR7 in 10% FBS and 10% NGS in PBS for 2.5 h at room temperature. The flat mounted retinas were photographed with a confocal laser scanning microscope system TCSSP™ (Leica).

Intensity index calculation

GFAP and FITC-dextran stained images were analyzed with ImageJ software (Version 1.44, NIH, Bethesda, MD). Each images were captured using the same camera settings for power, gain, iris aperture size. Data was obtained for the relative area of each region of interest with pixel intensity above a set threshold, and averaged across three

images for both of wild-type and mutant mice. Thus, the index of intensity is defined as the relative area of supra-threshold pixels in each region of interest averaged for both of wild-type and mutant mice (Feilchenfeld et al., 2008). All quantitation was performed with the experimenter blinded to the condition.

Statistical comparisons

All data were expressed as the mean ± standard deviation. For statistical comparisons of retinal thickness and amplitudes of a- and b-wave of ERGs, two-tailed Mann–Whitney nonparametric tests were used. For statistical comparisons of Intensity Index for GFAP immunoreactivity, unpaired t-tests were used. In all statistical comparisons, a P-value less than 0.05 was considered statistically significant.

Acknowledgments

We thank Dr. Duco Hamasaki for proofreading of our manuscript; Dr. Y.Oaki and other members of Department of Pathology, Nippon Medical School Chiba Hokusoh Hospital for the production of paraffin embedded mouse eyes; N.Asagawa for technical help for the production of retinal flat mounts. This work was supported by Grants-in-Aid for Scientific Research (18590392) from the Japanese Ministry of Education, Culture, Sports, Science and Technology. For Research on Psychiatric and Neurological Diseases and Mental Health (H20-016) and Nervous and Mental Disorders (19A-7) from the Japanese Ministry of Health, Labor and Welfare.

References

Beltrán-Valero de Bernabé, D., Currier, S., Steinbrecher, A., Celli, J., van Beusekom, E., van der Zwaag, B., Kayserili, H., Merlini, L., Chitayat, D., Dobyns, W.B., Cormand, B., Lehesjoki, A.E., Cruces, J., Voit, T., Walsh, C.A., van Bokhoven, H., Brunner, H.G., 2002. Mutations in the O-mannosyltransferase gene POMT1 give rise to the severe neuronal migration disorder Walker-Warburg syndrome. Am. J. Hum. Genet. 71, 1033–1043.

Blake, D.J., Kröger, S., 2000. The neurobiology of duchenne muscular dystrophy: learning lessons from muscle? Trends Neurosci. 23, 92–99.

Brockington, M., Blake, D.J., Prandini, P., Brown, S.C., Torelli, S., Benson, M.A., Ponting, C.P., Estournet, B., Romero, N.B., Mercuri, E., Voit, T., Sewry, C.A., Guicheney, P., Muntoni, F., 2001. Mutations in the fukutin-related protein gene (FKRP) cause a form of congenital muscular dystrophy with secondary laminin alpha2 deficiency and abnormal glycosylation of alpha-dystroglycan. Am. J. Hum. Genet. 69, 1198–1209.

Caicedo, A., Espinosa-Heidmann, D.G., Piña, Y., Hernandez, E.P., Cousins, S.W., 2005. Blood-derived macrophages infiltrate the retina and activate Müller glial cells under experimental choroidal neovascularization. Exp. Eye Res. 81, 38–47.

Chi, Zai-Long, Akahori, M., Obazawa, M., Minami, M., Noda, T., Nakaya, N., Tomarev, S., Kawase, K., Yamamoto, T., Noda, S., Sasaoka, M., Shimazaki, A., Takada, Y., Iwata, T., 2010. Overexpression of optineurin E50K disrupts Rab8 interaction and leads to a progressive retinal degeneration in mice. Hum. Mol. Genet. 19, 2606–2615.

Claudepierre, T., Rodius, F., Frasson, M., Fontaine, V., Picaud, S., Dreyfus, H., Mornet, D., Rendon, A., 1999. Differential distribution of dystrophins in rat retina. Invest. Ophthalmol. Vis. Sci. 40, 1520–1529.

Cormand, B., Pihko, H., Bayés, M., Valanne, L., Santavuori, P., Talim, B., Gershoni-Baruch, R., Ahmad, A., van Bokhoven, H., Brunner, H.G., Voit, T., Topaloglu, H., Dobyns, W.B., Lehesjoki, A.E., 2001. Clinical and genetic distinction between Walker-Warburg syndrome and muscle–eye–brain disease. Neurology 56, 1059–1069.

Dalloz, C., Sarig, R., Fort, P., Yaffe, D., Bordais, A., Pannicke, T., Grosche, J., Mornet, D., Reichenbach, A., Sahel, J., Nudel, U., Rendon, A., 2003. Targeted inactivation of dystrophin gene product Dp71: phenotypic impact in mouse retina. Hum. Mol. Genet. 12, 1543–1554.

Demir, E., Gucuyener, K., Akturk, A., Talim, B., Konus, O., Del Bo, R., Ghezzi, S., Comi, G.P., 2009. An unusual presentation of muscle–eye–brain disease: severe eye abnormalities with mild muscle and brain involvement. Neuromuscul. Disord. 19, 692–695.

Diesen, C., Saarinen, A., Pihko, H., Rosenlew, C., Cormand, B., Dobyns, W.B., Dieguez, J., Valanne, L., Joensuu, T., Lehesjoki, A.E., 2004. POMGnT1 mutation and phenotypic spectrum in muscle–eye–brain disease. J. Med. Genet. 41, e115.

Ervasti, J.M., Campbell, K.P., 1993. A role for the dystrophin–glycoprotein complex as a transmembrane linker between laminin and actin. J. Cell Biol. 122, 809–823.

Fahnehjelm, K.T., Ygge, J., Engman, M.L., Mosskin, M., Santavuori, P., Malm, G., 2001. A child with muscle–eye–brain disease. Ophthalmological and neurological characteristics. Acta Ophthalmol. Scand. 79, 72–75.

Feilchenfeld, Z., Yücel, Y.H., Gupta, N., 2008. Oxidative injury to blood vessels and glia of the pre-laminar optic nerve head in human glaucoma. Exp. Eye Res. 87, 409–414.

Fisher, S.K., Lewis, G.P., 2003. Müller cell and neuronal remodeling in retinal detachment and reattachment and their potential consequences for visual recovery: a review and reconsideration of recent data. Vision Res. 43, 887–897.

Fort, P.E., Sene, A., Pannicke, T., Roux, M.J., Forster, V., Mornet, D., Nudel, U., Yaffe, D., Reichenbach, A., Sahel, J.A., Rendon, A., 2008. Kir4.1 and AQP4 associate with Dp71- and utrophin-DAPs complexes in specific and defined microdomains of Müller retinal glial cell membrane. Glia 56, 597–610.

Gee, S.H., Montanaro, F., Lindenbaum, M.H., Carbonetto, S., 1994. Dystroglycan-alpha, a dystrophin-associated glycoprotein, is a functional agrin receptor. Cell 77, 675–686.

Godfrey, C., Clement, E., Mein, R., Brockington, M., Smith, J., Talim, B., Straub, V., Robb, S., Quinlivan, R., Feng, L., Jimenez-Mallebrera, C., Mercuri, E., Manzur, A.Y., Kinali, M., Torelli, S., Brown, S.C., Sewry, C.A., Bushby, K., Topaloglu, H., North, K., Abbs, S., Muntoni, F., 2007. Refining genotype phenotype correlations in muscular dystrophies with defective glycosylation of dystroglycan. Brain 130, 2725–2735.

Hehr, U., Uyanik, G., Gross, C., Walter, M.C., Bohring, A., Cohen, M., Oehl-Jaschkowitz, B., Bird, L.M., Shamdeen, G.M., Bogdahn, U., Schuierer, G., Topaloglu, H., Aigner, L., Lochmüller, H., Winkler, J., 2007. Novel POMGnT1 mutations define broader phenotypic spectrum of muscle–eye–brain disease. Neurogenetics 8, 279–288.

Henry, M.D., Campbell, K.P., 1999. Dystroglycan inside and out. Curr. Opin. Cell Biol. 11, 602–607.

Hu, H., Candiello, J., Zhang, P., Ball, S.L., Cameron, D.A., Halfter, W., 2010. Retinal ectopias and mechanically weakened basement membrane in a mouse model of muscle–eye–brain (MEB) disease congenital muscular dystrophy. Mol. Vis. 16, 1415–1428.

Ibraghimov-Beskrovnaya, O., Ervasti, J.M., Leveille, C.J., Slaughter, C.A., Sernett, S.W., Campbell, K.P., 1992. Primary structure of dystrophin-associated glycoproteins linking dystrophin to the extracellular matrix. Nature 355, 696–702.

Kameya, S., Araki, E., Katsuki, M., Mizota, A., Adachi, E., Nakahara, K., Nonaka, I., Sakuragi, S., Takeda, S., Nabeshima, Y., 1997. Dp260 disrupted mice revealed prolonged implicit time of the b-wave in ERG and loss of accumulation of beta-dystroglycan in the outer plexiform layer of the retina. Hum. Mol. Genet. 6, 2195–2203.

Kanagawa, M., Omori, Y., Sato, S., Kobayashi, K., Miyagoe-Suzuki, Y., Takeda, S., Endo, T., Furukawa, T., Toda, T., 2010. Post-translational maturation of dystroglycan is necessary for pikachurin binding and ribbon synaptic localization. J. Biol. Chem. 285, 31208–31216.

Kobayashi, K., Nakahori, Y., Miyake, M., Matsumura, K., Kondo-Iida, E., Nomura, Y., Segawa, M., Yoshioka, M., Saito, K., Osawa, M., Hamano, K., Sakakihara, Y., Nonaka, I., Nakagome, Y., Kanazawa, I., Nakamura, Y., Tokunaga, K., Toda, T., 1998. An ancient retrotransposal insertion causes Fukuyama-type congenital muscular dystrophy. Nature 394, 388–392.

Lee, Y., Kameya, S., Cox, G.A., Hsu, J., Hicks, W., Maddatu, T.P., Smith, R.S., Naggert, J.K., Peachey, N.S., Nishina, P.M., 2005. Ocular abnormalities in Large(myd) and Large (vls) mice, spontaneous models for muscle, eye, and brain diseases. Mol. Cell. Neurosci. 30, 160–172.

Lewis, G.P., Fisher, S.K., 2003. Up-regulation of glial fibrillary acidic protein in response to retinal injury: its potential role in glial remodeling and a comparison to vimentin expression. Int. Rev. Cytol. 230, 263–290.

Lewis, G.P., Matsumoto, B., Fisher, S.K., 1995. Changes in the organization and expression of cytoskeletal proteins during retinal degeneration induced by retinal detachment. Invest. Ophthalmol. Vis. Sci. 36, 2404–2416.

Liu, J., Ball, S.L., Yang, Y., Mei, P., Zhang, L., Shi, H., Kaminski, H.J., Lemmon, V.P., Hu, H., 2006. A genetic model for muscle–eye–brain disease in mice lacking protein O-mannose 1,2-N-acetylglucosaminyltransferase (POMGnT1). Mech. Dev. 123, 228–240.

Longman, C., Brockington, M., Torelli, S., Jimenez-Mallebrera, C., Kennedy, C., Khalil, N., Feng, L., Saran, R.K., Voit, T., Merlini, L., Sewry, C.A., Brown, S.C., Muntoni, F., 2003. Mutations in the human LARGE gene cause MDC1D, a novel form of congenital muscular dystrophy with severe mental retardation and abnormal glycosylation of alpha-dystroglycan. Hum. Mol. Genet. 12, 2853–2861.

MacLaren, R.E., 1996. Development and role of retinal glia in regeneration of ganglion cells following retinal injury. Br. J. Ophthalmol. 80, 458–464.

Matsumoto, H., Hayashi, Y.K., Kim, D.S., Ogawa, M., Murakami, T., Noguchi, S., Nonaka, I., Nakazawa, T., Matsuo, T., Futagami, S., Campbell, K.P., Nishino, I., 2005. Congenital muscular dystrophy with glycosylation defects of alpha-dystroglycan in Japan. Neuromuscul. Disord. 15, 342–348.

Mercuri, E., Messina, S., Bruno, C., Mora, M., Pegoraro, E., Comi, G.P., D'Amico, A., Aiello, C., Biancheri, R., Berardinelli, A., Boffi, P., Cassandrini, D., Laverda, A., Moggio, M., Morandi, L., Moroni, I., Pane, M., Pezzani, R., Pichiecchio, A., Pini, A., Minetti, C., Mongini, T., Mottarelli, E., Ricci, E., Ruggieri, A., Saredi, S., Scuderi, C., Tessa, A., Toscano, A., Tortorella, G., Trevisan, C.P., Uggetti, C., Vasco, G., Santorelli, F.M., Bertini, E., 2009. Congenital muscular dystrophies with defective glycosylation of dystroglycan: a population study. Neurology 72, 1802–1809.

Miyagoe-Suzuki, Y., Masubuchi, N., Miyamoto, K., Wada, M.R., Yuasa, S., Saito, F., Matsumura, K., Kanesaki, H., Kudo, A., Manya, H., Endo, T., Takeda, S., 2009. Reduced proliferative activity of primary POMGnT1-null myoblasts in vitro. Mech. Dev. 126, 107–116.

Mizutani, M., Gerhardinger, C., Lorenzi, M., 1998. Müller cell changes in human diabetic retinopathy. Diabetes 47, 445–449.

Montanaro, F., Carbonetto, S., Campbell, K.P., Lindenbaum, M., 1995. Dystroglycan expression in the wild type and mdx mouse neural retina: synaptic colocalization with dystrophin, dystrophin-related protein but not laminin. J. Neurosci. Res. 42, 528–538.

Peng, H.B., Ali, A.A., Daggett, D.F., Rauvala, H., Hassell, J.R., Smalheiser, N.R., 1998. The relationship between perlecan and dystroglycan and its implication in the formation of the neuromuscular junction. Cell Adhes. Commun. 5, 475–489.

Pihko, H., Lappi, M., Raitta, C., Sainio, K., Valanne, L., Somer, H., Santavuori, P., 1995. Ocular findings in muscle–eye–brain (MEB) disease: a follow-up study. Brain Dev. 17, 57–61.

Pillers, D.A., Bulman, D.E., Weleber, R.G., Sigesmund, D.A., Musarella, M.A., Powell, B.R., Murphey, W.H., Westall, C., Panton, C., Becker, L.E., Worton, R.G., Ray, P.N., 1993. Dystrophin expression in the human retina is required for normal function as defined by electroretinography. Nat. Genet. 4, 82–86.

Pillers, D.A., Weleber, R.G., Woodward, W.R., Green, D.G., Chapman, V.M., Ray, P.N., 1995. mdxCv3 mouse is a model for electroretinography of Duchenne/Becker muscular dystrophy. Invest. Ophthalmol. Vis. Sci. 36, 462–466.

Pillers, D.A., Fitzgerald, K.M., Duncan, N.M., Rash, S.M., White, R.A., Dwinnell, S.J., Powell, B.R., Schnur, R.E., Ray, P.N., Cibis, G.W., Weleber, R.G., 1999. Duchenne/Becker muscular dystrophy: correlation of phenotype by electroretinography with sites of dystrophin mutations. Hum. Genet. 105, 2–9.

Sato, S., Omori, Y., Katoh, K., Kondo, M., Kanagawa, M., Miyata, K., Funabiki, K., Koyasu, T., Kajimura, N., Miyoshi, T., Sawai, H., Kobayashi, K., Tani, A., Toda, T., Usukura, J., Tano, Y., Fujikado, T., Furukawa, T., 2008. Pikachurin, a dystroglycan ligand, is essential for photoreceptor ribbon synapse formation. Nat. Neurosci. 11, 923–931.

Satz, J.S., Philp, A.R., Nguyen, H., Kusano, H., Lee, J., Turk, R., Riker, M.J., Hernández, J., Weiss, R.M., Anderson, M.G., Mullins, R.F., Moore, S.A., Stone, E.M., Campbell, K.P., 2009. Visual impairment in the absence of dystroglycan. J. Neurosci. 29, 13136–13146.

Straub, V., Campbell, K.P., 1997. Muscular dystrophies and the dystrophin–glycoprotein complex. Curr. Opin. Neurol. 10, 168–175.

Sugita, S., Saito, F., Tang, J., Satz, J., Campbell, K.P., Südhof, T.C., 2001. A stoichiometric complex of neurexins and dystroglycan in brain. J. Cell Biol. 154, 435–445.

Takeda, S., Kondo, M., Sasaki, J., Kurahashi, H., Kano, H., Arai, K., Misaki, K., Fukui, T., Kobayashi, K., Tachikawa, M., Imamura, M., Nakamura, Y., Shimizu, T., Murakami, T., Sunada, Y., Fujikado, T., Matsumura, K., Terashima, T., Toda, T., 2003. Fukutin is required for maintenance of muscle integrity, cortical histiogenesis and normal eye development. Hum. Mol. Genet. 12, 1449–1459.

Ueda, H., Kobayashi, T., Mitsui, K., Tsurugi, K., Tsukahara, S., Ohno, S., 1995. Dystrophin localization at presynapse in rat retina revealed by immunoelectron microscopy. Invest. Ophthalmol. Vis. Sci. 36, 2318–2322.

van Reeuwijk, J., Janssen, M., van den Elzen, C., Beltran-Valero de Bernabé, D., Sabatelli, P., Merlini, L., Boon, M., Scheffer, H., Brockington, M., Muntoni, F., Huynen, M.A., Verrips, A., Walsh, C.A., Barth, P.G., Brunner, H.G., van Bokhoven, H., 2005. POMT2 mutations cause alpha-dystroglycan hypoglycosylation and Walker-Warburg syndrome. J. Med. Genet. 42, 907–912.

Yang, Y., Zhang, P., Xiong, Y., Li, X., Qi, Y., Hu, H., 2007. Ectopia of meningeal fibroblasts and reactive gliosis in the cerebral cortex of the mouse model of muscle–eye–brain disease. J. Comp. Neurol. 505, 459–477.

Yoshida, A., Kobayashi, K., Manya, H., Taniguchi, K., Kano, H., Mizuno, M., Inazu, T., Mitsuhashi, H., Takahashi, S., Takeuchi, M., Herrmann, R., Straub, V., Talim, B., Voit, T., Topalogu, H., Toda, T., Endo, T., 2001. Muscular dystrophy and neuronal migration disorder caused by mutation in a glycosyltransferase, POMGnT1. Dev. Cell 1, 717–724.